LETTERS

Nicotine binding to brain receptors requires a strong cation–π interaction

Xinan Xiu[1]*, Nyssa L. Puskar[1]*, Jai A. P. Shanata[1], Henry A. Lester[2] & Dennis A. Dougherty[1]

Nicotine addiction begins with high-affinity binding of nicotine to acetylcholine (ACh) receptors in the brain. The end result is over 4,000,000 smoking-related deaths annually worldwide and the largest source of preventable mortality in developed countries. Stress reduction, pleasure, improved cognition and other central nervous system effects are strongly associated with smoking. However, if nicotine activated ACh receptors found in muscle as potently as it does brain ACh receptors, smoking would cause intolerable and perhaps fatal muscle contractions. Despite extensive pharmacological, functional and structural studies of ACh receptors, the basis for the differential action of nicotine on brain compared with muscle ACh receptors has not been determined. Here we show that at the α4β2 brain receptors thought to underlie nicotine addiction, the high affinity for nicotine is the result of a strong cation–π interaction to a specific aromatic amino acid of the receptor, TrpB. In contrast, the low affinity for nicotine at the muscle-type ACh receptor is largely due to the fact that this key interaction is absent, even though the immediate binding site residues, including the key amino acid TrpB, are identical in the brain and muscle receptors. At the same time a hydrogen bond from nicotine to the backbone carbonyl of TrpB is enhanced in the neuronal receptor relative to the muscle type. A point mutation near TrpB that differentiates α4β2 and muscle-type receptors seems to influence the shape of the binding site, allowing nicotine to interact more strongly with TrpB in the neuronal receptor. ACh receptors are established therapeutic targets for Alzheimer's disease, schizophrenia, Parkinson's disease, smoking cessation, pain, attention-deficit hyperactivity disorder, epilepsy, autism and depression[1]. Along with solving a chemical mystery in nicotine addiction, our results provide guidance for efforts to develop drugs that target specific types of nicotinic receptors.

Nicotinic acetylcholine receptors (nAChRs) comprise a family of ≥20 homologous subtypes that mediate fast synaptic transmission throughout the central and peripheral nervous systems[2]. The neuronal receptors are found in the central nervous system (CNS) and autonomic ganglia. Of these, the subtype most strongly associated with nicotine addiction and the target of recently developed smoking cessation drugs is termed α4β2 (refs 3–7). The high nicotine affinity of α4β2 receptors, when combined with the ability of nicotine to cross the blood–brain barrier and its favourable pharmacokinetics, allows nicotine at the submicromolar concentrations in tobacco smoke to activate acutely these receptors, providing reward, cognitive sensitization and perhaps other effects. In addition, the high-affinity interaction allows smoked nicotine to act as an intracellular pharmacological chaperone of α4β2 receptors, leading to the upregulation of receptors thought to underlie effects of chronic exposure[6,8].

In previous studies of the nAChR of the neuromuscular junction (muscle type), we showed that an important contributor to ACh binding is a cation–π interaction to a specific tryptophan (called TrpB, residue 149, Fig. 1)[9]. These results were subsequently supported by the important series of crystal structures of ACh binding proteins (AChBP)[10,11]. These structures revealed the 'aromatic box' structural motif of Fig. 1, and the aligning residues are predominantly aromatic throughout the Cys-loop family of neurotransmitter-gated ion channels. In other Cys-loop receptors, a cation–π interaction between the natural agonist and one of the aromatics is always seen, although its precise location varies[12]. Interestingly, when nicotine activates the muscle-type nAChR, there is no cation–π interaction[13], consistent with its relatively low affinity for this receptor. This suggested that a cation–π interaction could discriminate between high-affinity neuronal receptors and low-affinity muscle-type receptors. However, subtle effects must be involved, as the nAChRs of the CNS and neuromuscular junction are homologous throughout most regions of sequence and are essentially identical in the immediate vicinity of the agonist binding site (Supplementary Fig. 1).

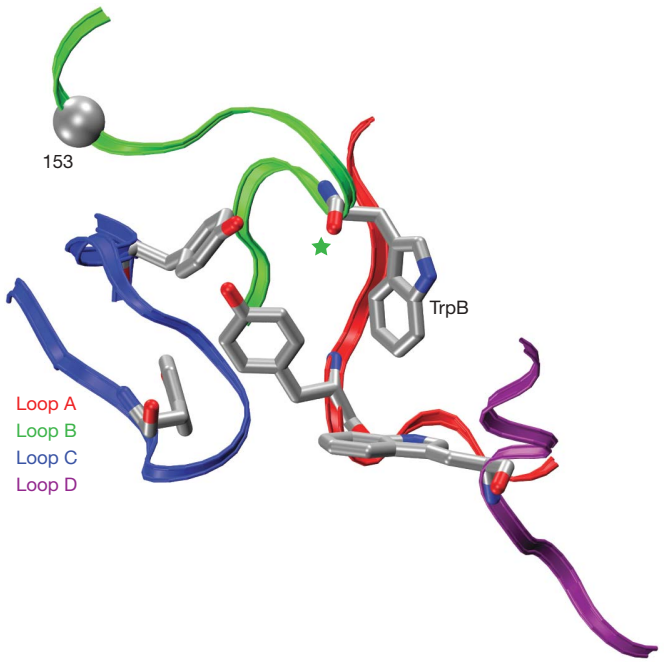

Figure 1 | The binding site of AChBP, thought to resemble that of nAChRs. Shown are the four principal 'loops' that define the binding site[2]. Also highlighted are TrpB (149) studied here; its backbone carbonyl (green star); and the α carbon on position 153, which has also been mutated here. Note that loop C contributes two aromatic residues; the other loops each contribute one. The image is of Protein Data Bank file 1I9B (ref. 10).

[1]Divisions of Chemistry and Chemical Engineering and [2]Biology, California Institute of Technology, 1200 East California Boulevard, Pasadena, California 91125, USA.
*These authors contributed equally to this work.

Here we describe studies of the α4β2 neuronal receptor. We find a remarkable alteration of binding behaviour: both ACh and nicotine make a strong cation–π interaction to TrpB. In addition, a hydrogen bond from nicotine to the backbone carbonyl of TrpB that is weak in the muscle-type is much stronger in the α4β2 receptor. Taken together, these two noncovalent interactions fully rationalize the differential affinity of nicotine in the brain versus the neuromuscular junction.

A cation–π interaction between a drug and a receptor can be revealed by incorporation of a series of fluorinated amino acid analogues (Fig. 2); a consistent trend in receptor response indicates a binding interaction. Such an experiment is enabled by the nonsense suppression methodology for incorporation of unnatural amino acids into receptors and channels expressed in *Xenopus* oocytes. Although we have found the nonsense suppression methodology to be broadly applicable[14,15], implementing the methodology for study of the α4β2 neuronal nAChRs proved to be especially challenging, requiring new strategies. The α4β2 receptors are expressed in *Xenopus* oocytes at inadequately low levels for nonsense suppression experiments. However, recent studies showed that the Leu9′Ala (L9′A) mutation in the M2 transmembrane helix of the α4 subunit greatly improves expression without altering the pharmacological selectivity of the receptor[16]. (In Cys-loop receptors, the highly homologous M2 sequences are often compared by numbering from the cytoplasmic end, termed position 1′.) Therefore, all studies of α4β2 described here included this mutation. As with other mutations of L9′, the L9′A mutation lowers the agonist concentration for half-maximum response (EC_{50}) by influencing receptor gating in ways that are fairly well understood and that do not distort the present analysis of the binding site (some 60 Å from the 9′ position)[17,18]. In addition, previous studies of the muscle-type receptor used a comparable mutation at L9′, and control experiments established that it did not alter binding trends[9,19].

The nAChRs are pentameric. The muscle-type receptor has a precise stoichiometry of $(\alpha1)_2\beta1\gamma\delta$. However, the α4β2 receptor can have variable stoichiometry. In particular, there are two forms of α4β2, $(\alpha4)_2(\beta2)_3$ and $(\alpha4)_3(\beta2)_2$, which we refer to hereafter as A2B3 and A3B2, respectively[8,20,21]. Agonist binding sites are at the appropriate α–β interfaces. The A2B3 form has higher sensitivity for nicotine and may be upregulated during chronic exposure to nicotine; our studies have focused on it. Controlling the ratios of messenger RNAs injected into the oocyte can reliably control subunit stoichiometry in the wild-type receptor. However, in a nonsense suppression experiment, the subunit that contains the stop codon where the unnatural amino acid has been incorporated can show low and variable expression levels. Therefore we sought a second, independent indicator of the stoichiometry of the α4β2 receptor. We now report that the A2B3 and A3B2 forms of the α4(L9′A)β2 receptor show markedly different rectification behaviours. As indicated by either voltage ramp or voltage jump experiments, A2B3 is substantially more inward rectifying than A3B2 (Supplementary Fig. 2). Thus, in all our experiments with unnatural amino acids, the stoichiometries of mutant receptors are monitored by measuring current–voltage relations with voltage jumps. For each mutant receptor studied, we determined the fraction (outward current at +70 mV/inward current at –110 mV), and a value ≤0.1 establishes the desired A2B3 stoichiometry (Supplementary Table 1 and Supplementary Discussion). With these methodological developments in hand, incorporation of unnatural amino acids into the α4β2 receptor becomes feasible (Fig. 3).

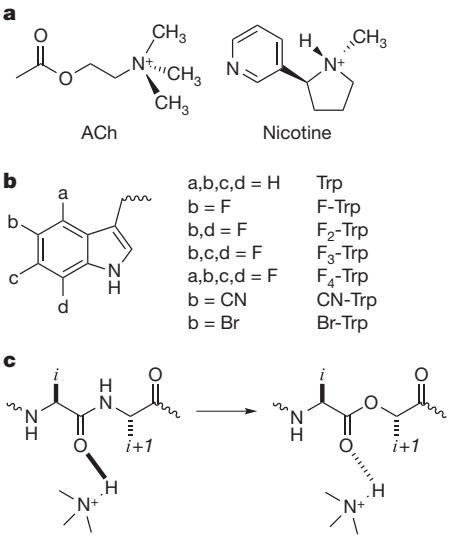

Figure 2 | Agonists and unnatural amino acids considered here. **a**, Structures of ACh and nicotine. **b**, Unnatural amino acids considered here. If not indicated, an a, b, c, or d group is H. Br, bromo group; CN, cyano group. **c**, The backbone ester strategy for modulating a hydrogen bond.

As shown in Supplementary Table 1 and Fig. 4, a compelling 'fluorination' trend is seen for both ACh and nicotine at TrpB of the α4β2 receptor. This is in contrast to the results at the muscle-type receptor, in which no such trend is seen for nicotine activation. Further support for an important cation–π interaction for both agonists is provided by the large perturbation induced by a cyano (CN) group—which is strongly deactivating in a cation–π interaction—compared to a bromo (Br) group, which is roughly isosteric to a cyano group but much less deactivating.

We have also evaluated other residues that constitute the aromatic box of the ACh binding site (Supplementary Table 1). The results for α4β2 very much parallel our previous findings for the muscle-type receptor (Supplementary Discussion). This indicates that it is specifically the interaction with TrpB that discriminates the two receptor subtypes.

The EC_{50} values reported here represent a measure of receptor function; shifts in EC_{50} can result from changes in ligand binding and/or receptor gating properties. By ascribing the results to attenuation of a cation–π interaction, we are effectively concluding that it is ligand binding that is being modulated by fluorination, but that conclusion is not incontrovertible. To resolve this ambiguity, we evaluated the gating behaviours of key receptors using single-channel recording. For the wild type and the receptor with 5,6,7-trifluorotryptophan (F_3-Trp) at TrpB, we compared the probabilities that the channel is open (P_{open}) at nicotine concentrations that evoke half-maximal macroscopic steady-state currents (EC_{50} = 0.08 μM and 1.2 μM, respectively). Any differences between the two P_{open} values must result from differences in gating behaviours. As suggested by Fig. 5 and as confirmed by further single-channel analysis (Supplementary Fig. 3 and Supplementary Discussion), the wild-type and mutant receptors have P_{open} values that are essentially indistinguishable. Thus, the shift in EC_{50} for F_3-Trp is primarily, if not exclusively, a consequence of changes in binding. Fluorination of TrpB of the α4β2 (A2B3) receptor primarily has an impact on the sensitivity to nicotine by decreasing nicotine's cation–π interaction with this residue.

These results indicate that nicotine is positioned more closely to TrpB in the α4β2 agonist binding site than in the muscle type. This suggested that another nicotine-binding interaction could also be altered. An important chemical distinction between ACh and nicotine is that only the latter can act as a hydrogen bond donor, through the pyrrolidine N^+-H (Fig. 2a). Examination of the AChBP crystal structures (Fig. 1)[22] suggested that the backbone carbonyl associated with TrpB could act as the hydrogen bond acceptor, and several groups have shown the importance of this interaction[22–24]. Previously, we probed this potential hydrogen bond in the muscle-type receptor by replacing the $(i+1)$ residue with its α-hydroxy analogue (Fig. 2c). This converts the backbone amide to a backbone ester, which is well established to be a substantially poorer hydrogen bond acceptor. In the muscle-type receptor, this change raised the

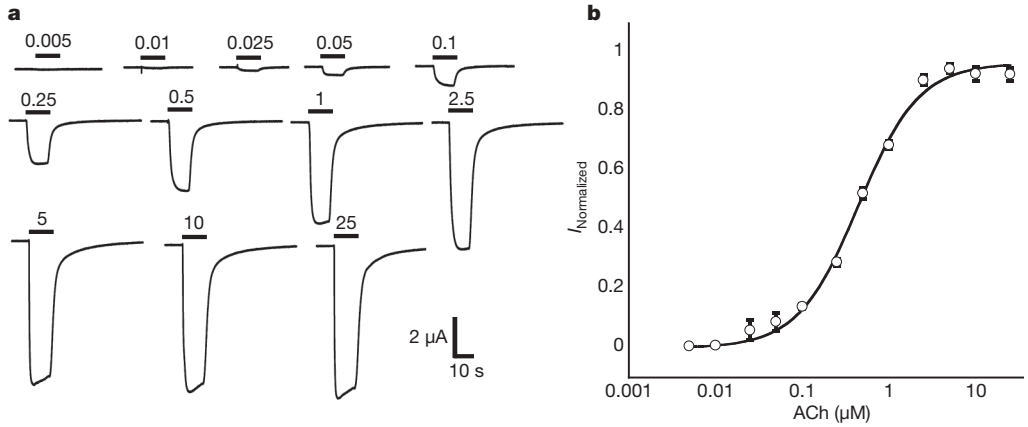

Figure 3 | Nonsense suppression in the α4β2 receptor. Shown is a wild-type recovery experiment, in which Trp is incorporated at the TrpB position. **a**, Representative traces of voltage-clamp currents. Bars represent application of ACh at concentrations noted. **b**, Fit of data in **a** to the Hill equation. Error bars indicate s.e.m.; $n = 6–8$.

nicotine EC_{50} by a modest factor of 1.6 (ref. 25). We now find that for precisely the same change in the α4β2 receptor, the nicotine EC_{50} increases 19-fold, a relatively large effect for such a subtle mutation[26–28]. Recall that the backbone ester substitution does not destroy the hydrogen bond, it simply attenuates it. Notably, ACh, which cannot make a conventional hydrogen bond to the carbonyl, shows no shift in EC_{50} in response to this mutation (Supplementary Table 1).

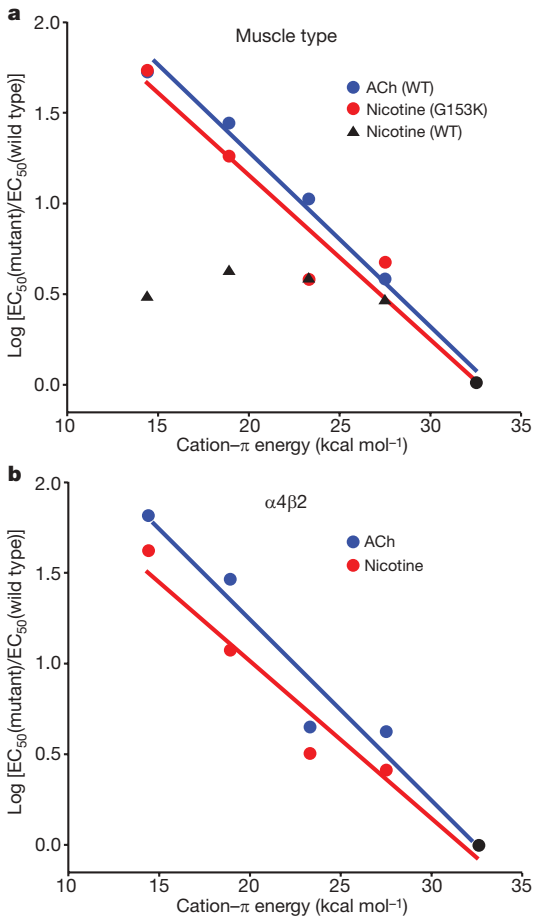

Figure 4 | Fluorination plots. Note that in both plots, all data sets share the point at $x = 32.6$ kcal mol^{-1} (cation–π energy for Trp); $y = 0$ (black circle). Moving to the left then corresponds to monofluoro-, difluoro-, trifluoro- and tetrafluoro-TrpB. Cation–π binding energies (x axes) are from ref. 9. **a**, Muscle-type receptor. The designation WT indicates Gly at position 153. **b**, α4β2 receptor.

This establishes that the ester mutation does not globally alter the binding/gating characteristics of the receptor.

The differential affinity of nicotine for α4β2 versus muscle-type receptors results from stronger interactions in the former with TrpB—both cation–π and hydrogen bonding. Because the two receptors are identical with regard to the five residues that make up the aromatic box, a factor 'outside the box' must be influencing its precise geometry, such that nicotine can approach TrpB more closely in α4β2 than in muscle-type nAChR. Pioneering work has identified residues responsible for the fact that α4β2 receptors show consistently higher affinity than the homopentameric α7 neuronal receptors[29]. At a particular residue in loop B—position 153, just four residues from TrpB—mutations strongly influence affinity. In high-affinity α4β2 receptors this residue is a Lys, and this residue is proposed to help shape the aromatic box by forming a backbone hydrogen bond between loops B and C (Fig. 1). In the lower affinity α7 neuronal receptor, residue 153 is a Gly, and molecular dynamics simulations of α7 suggest that a Gly at 153 discourages the formation of the hydrogen bond between loops B and C. Interestingly, the aligned residue in the muscle-type receptor is also Gly, and a naturally occurring G153S mutation is gain-of-function and associated with a congenital myasthenic syndrome[30]. We now report that the muscle-type α1 G153K mutant shows much higher affinity for nicotine, and that, when this mutation is present, the cation–π

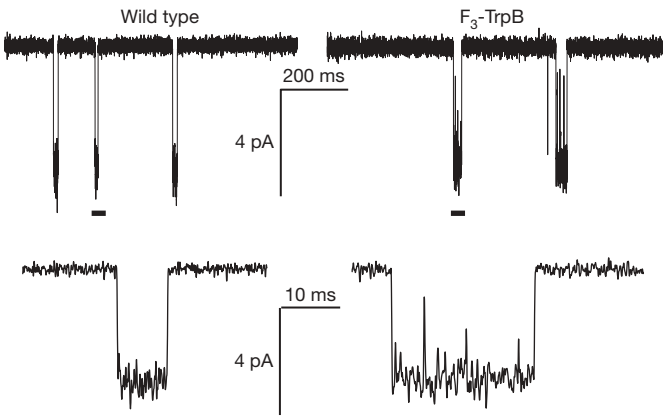

Figure 5 | Single-channel recordings from wild-type α4β2 (conventional expression) and the F_3-Trp mutant (nonsense suppression) at site B, with nicotine applied at EC_{50} values (0.080 and 1.2 μM, respectively). Lower traces are expansions of the regions marked by a bar in the upper trace. Records were obtained in the cell-attached configuration with a pipette potential of +100 mV and are shown at 2 kHz bandwidth. Channel openings are shown as downward deflections.

interaction to TrpB is strong. The data are summarized in Supplementary Table 1 and Fig. 4. As expected, the ACh cation–π interaction is maintained in the muscle-type receptor with the G153K mutation. These data indicate that the loop B–loop C hydrogen bond that is naturally present in α4β2 shapes the aromatic box so that nicotine can make a closer contact to TrpB, and that this structural feature is absent or weaker in the muscle-type receptor.

Taken together, the present results indicate that the higher affinity of nicotine in the brain relative to the neuromuscular junction is a consequence of enhanced interactions with TrpB. A cation–π interaction that is absent in the muscle-type receptor is quite strong in α4β2. In addition, a hydrogen bond to a backbone carbonyl that is weak in the muscle type is enhanced in α4β2. Both effects are quite substantial, and in combination they are more than adequate to account fully for the differential sensitivity to nicotine of the two receptors. The side chain of residue 153 in loop B distinguishes the two receptor types and apparently influences the shape of the binding site aromatic box, allowing a stronger interaction between nicotine and TrpB in high-affinity receptors.

METHODS SUMMARY

Whole-cell electrophysiological characterization of agonist-induced responses. Rat α4β2 and mouse $(\alpha1)_2\beta1\gamma\delta$ ion channels were expressed in *Xenopus laevis* oocytes. For α4β2 receptors, subunit stoichiometry was controlled by varying the α4:β2 subunit ratio and verified by voltage-jump experiments. Dose–response measurements for these channels were performed with a holding potential of −60 mV.

Unnatural amino acid/α-hydroxy acid incorporation. Unnatural amino acids and α-hydroxy acids were prepared, coupled to dCA and ligated to 74-mer THG73 as described previously[15].

Single-channel characterization of α4β2. Single-channel recording was performed in the cell-attached configuration with a pipette potential of +100 mV as described previously[27]. P_{open} values were calculated from event-detected data using Clampfit 9.2 single-channel search.

See associated *Nature Protocols* paper by X.X. *et al.* (in the press).

Full Methods and any associated references are available in the online version of the paper at www.nature.com/nature.

Received 26 November 2008; accepted 9 January 2009.
Published online 1 March 2009.

1. Romanelli, M. N. *et al.* Central nicotinic receptors: structure, function, ligands, and therapeutic potential. *ChemMedChem* **2,** 746–767 (2007).
2. Corringer, P. J., Le Novere, N. & Changeux, J. P. Nicotinic receptors at the amino acid level. *Annu. Rev. Pharmacol. Toxicol.* **40,** 431–458 (2000).
3. Coe, J. W. *et al.* Varenicline: An α4β2 nicotinic receptor partial agonist for smoking cessation. *J. Med. Chem.* **48,** 3474–3477 (2005).
4. Gotti, C., Zoli, M. & Clementi, F. Brain nicotinic acetylcholine receptors: native subtypes and their relevance. *Trends Pharmacol. Sci.* **27,** 482–491 (2006).
5. Mansvelder, H. D., Keath, J. R. & McGehee, D. S. Synaptic mechanisms underlie nicotine-induced excitability of brain reward areas. *Neuron* **33,** 905–919 (2002).
6. Nashmi, R. *et al.* Chronic nicotine cell specifically upregulates functional α4* nicotinic receptors: basis for both tolerance in midbrain and enhanced long-term potentiation in perforant path. *J. Neurosci.* **27,** 8202–8218 (2007).
7. Tapper, A. R. *et al.* Nicotine activation of α4* receptors: sufficient for reward, tolerance, and sensitization. *Science* **306,** 1029–1032 (2004).
8. Kuryatov, A., Luo, J., Cooper, J. & Lindstrom, J. Nicotine acts as a pharmacological chaperone to up-regulate human α4β2 acetylcholine receptors. *Mol. Pharm.* **68,** 1839–1851 (2005).
9. Zhong, W. *et al.* From *ab initio* quantum mechanics to molecular neurobiology: A cation-π binding site in the nicotinic receptor. *Proc. Natl Acad. Sci. USA* **95,** 12088–12093 (1998).
10. Brejc, K. *et al.* Crystal structure of an ACh-binding protein reveals the ligand-binding domain of nicotinic receptors. *Nature* **411,** 269–276 (2001).
11. Sixma, T. K. & Smit, A. B. Acetylcholine binding protein (AChBP): a secreted glial protein that provides a high-resolution model for the extracellular domain of pentameric ligand-gated ion channels. *Annu. Rev. Biophys. Biomol. Struct.* **32,** 311–334 (2003).
12. Dougherty, D. A. Cys-loop neuroreceptors: structure to the rescue? *Chem. Rev.* **108,** 1642–1653 (2008).
13. Beene, D. L. *et al.* Cation-π interactions in ligand recognition by serotonergic ($5\text{–}HT_{3A}$) and nicotinic acetylcholine receptors: The anomalous binding properties of nicotine. *Biochemistry* **41,** 10262–10269 (2002).
14. Dougherty, D. A. Physical organic chemistry on the brain. *J. Org. Chem.* **73,** 3667–3673 (2008).
15. Nowak, M. W. *et al. In vivo* incorporation of unnatural amino acids into ion channels in a *Xenopus* oocyte expression system. *Methods Enzymol.* **293,** 504–529 (1998).
16. Fonck, C. *et al.* Novel seizure phenotype and sleep disruptions in knock-in mice with hypersensitive α4* nicotinic receptors. *J. Neurosci.* **25,** 11396–11411 (2005).
17. Filatov, G. N. & White, M. M. The role of conserved leucines in the M2 domain of the acetylcholine receptor in channel gating. *Mol. Pharmacol.* **48,** 379–384 (1995).
18. Labarca, C. *et al.* Channel gating governed symmetrically by conserved leucine residues in the M2 domain of nicotinic receptors. *Nature* **376,** 514–516 (1995).
19. Kearney, P. *et al.* Dose-response relations for unnatural amino acids at the agonist binding site of the nicotinic acetylcholine receptor: Tests with novel side chains and with several agonists. *Mol. Pharmacol.* **50,** 1401–1412 (1996).
20. Moroni, M., Zwart, R., Sher, E., Cassels, B. K. & Bermudez, I. α4β2 nicotinic receptors with high and low acetylcholine sensitivity: pharmacology, stoichiometry, and sensitivity to long-term exposure to nicotine. *Mol. Pharmacol.* **70,** 755–768 (2006).
21. Nelson, M. E., Kuryatov, A., Choi, C. H., Zhou, Y. & Lindstrom, J. Alternate stoichiometries of α4β2 nicotinic acetylcholine receptors. *Mol. Pharmacol.* **63,** 332–341 (2003).
22. Celie, P. H. *et al.* Nicotine and carbamylcholine binding to nicotinic acetylcholine receptors as studied in AChBP crystal structures. *Neuron* **41,** 907–914 (2004).
23. Hansen, S. B. *et al.* Structures of aplysia AChBP complexes with nicotinic agonists and antagonists reveal distinctive binding interfaces and conformations. *EMBO J.* **24,** 3635–3646 (2005).
24. Talley, T. T. *et al.* Spectroscopic analysis of benzylidene anabaseine complexes with acetylcholine binding proteins as models for ligand-nicotinic receptor interactions. *Biochemistry* **45,** 8894–8902 (2006).
25. Cashin, A. L., Petersson, E. J., Lester, H. A. & Dougherty, D. A. Using physical chemistry to differentiate nicotinic from cholinergic agonists at the nicotinic acetylcholine receptor. *J. Am. Chem. Soc.* **127,** 350–356 (2005).
26. Deechongkit, S. *et al.* Context-dependent contributions of backbone hydrogen bonding to β-sheet folding energetics. *Nature* **430,** 101–105 (2004).
27. England, P. M., Zhang, Y., Dougherty, D. A. & Lester, H. A. Backbone mutations in transmembrane domains of a ligand-gated ion channel: implications for the mechanism of gating. *Cell* **96,** 89–98 (1999).
28. Koh, J. T., Cornish, V. W. & Schultz, P. G. An experimental approach to evaluating the role of backbone interactions in proteins using unnatural amino acid mutagenesis. *Biochemistry* **36,** 11314–11322 (1997).
29. Grutter, T. *et al.* An H-bond between two residues from different loops of the acetylcholine binding site contributes to the activation mechanism of nicotinic receptors. *EMBO J.* **22,** 1990–2003 (2003).
30. Sine, S. M. *et al.* Mutation of the acetylcholine receptor α subunit causes a slow-channel myasthenic syndrome by enhancing agonist binding affinity. *Neuron* **15,** 229–239 (1995).

Supplementary Information is linked to the online version of the paper at www.nature.com/nature.

Acknowledgements We thank B. N. Cohen for advice on single-channel recording and analysis. This work was supported by the NIH (NS 34407; NS 11756) and the California Tobacco-Related Disease Research Program of the University of California, grant number 16RT-0160. J.A.P.S. was partially supported by an NRSA training grant.

Author Information Reprints and permissions information is available at www.nature.com/reprints. Correspondence and requests for materials should be addressed to D.A.D. (dadougherty@caltech.edu).

METHODS

Whole-cell electrophysiological characterizations of the agonist-induced responses. Rat α4 and β2 mRNAs as well as mouse α1, β1(L9′S), γ and δ mRNAs were obtained from NotI linearizations of the expression vector pAMV, followed by *in vitro* transcription using the mMessage mMachine T7 kit (Ambion). The mutations for each subunit were introduced according to the QuikChange mutagenesis protocol (Stratagene).

To express wild-type neuronal ion channels, α4L9′A mRNA was co-injected with β2 mRNA at various ratios (total mRNA 10–25 ng cell^{-1}). Stage V–VI *Xenopus laevis* oocytes were injected and incubated at 18 °C for 24–48 h (whole-cell recording) or 60–90 h (single-channel recording).

Agonist-induced currents were recorded in two-electrode voltage clamp mode using the OpusXpress 6000A (Molecular Devices Axon Instruments) at a holding potential of −60 mV. Agonists were prepared in Ca^{2+}-free ND96 solution and applied for 12 s followed by a 2 min wash with Ca^{2+}-free ND96 solution between each agonist application. Acetylcholine chloride and (-)-nicotine tartrate were purchased from Sigma/Aldrich/RBI. Dose–response data were obtained for ≥6 concentrations of agonist and for ≥5 oocytes. Mutants with I_{max} of ≥100 nA were defined as functional. EC_{50} values and the Hill coefficient were calculated by fitting the dose–response relation to the Hill equation. All data are reported as mean ± s.e.m.

Voltage jump experiments were performed in the absence of ACh and also at EC_{50} concentration of ACh. The membrane potential was held at −60 mV, and stepped to 10 test potentials at 20-mV increments between +70 mV and −110 mV for 400 ms each. The voltage was then held for 600 ms at −60 mV holding potential between each episode. To isolate the ACh-induced currents, control traces ([ACh] = 0) were subtracted from the steady-state amplitudes of the ACh-induced currents of the test pulses. Normalized current–voltage curves were generated using current amplitudes normalized to that at −110 mV. For each α4L9′Aβ2 mutant, normalized $I_{+70\,mV}$ ± s.e.m. from ≥5 cells was reported.

Unnatural amino acid/α-hydroxy acid incorporation. Nitroveratryloxycarbonyl (NVOC) protected cyanomethyl ester forms of unnatural amino acids and α-hydroxythreonine cyanomethyl ester were synthesized, coupled to the dinucleotide dCA, and enzymatically ligated to 74-mer THG73 $tRNA_{CUA}$[15]. The unnatural amino-acid-conjugated tRNA was deprotected by photolysis immediately before co-injection with mRNA containing the UAG mutation at the site of interest. Approximately 10–25 ng mRNA and 25 ng tRNA-amino acid or tRNA-hydroxy acid were injected into stage V–VI oocytes in a total volume of 70 nl. For unnatural amino acid mutagenesis experiments in the muscle-type receptor, the α1, β1, γ and δ subunits were co-injected in a 10:1:1:1 ratio. All muscle-type receptors contained a L9′S mutation in the β subunit.

The fidelity of unnatural amino acid incorporation was confirmed at each site with a 'wild-type recovery' experiment and a 'read-through/reaminoacylation' test. In the wild-type recovery experiment, UAG mutant mRNA was co-injected with tRNA charged with the amino acid that is present at this site in the wild-type protein. Generation of receptors that were indistinguishable from the wild-type protein indicated that the residue carried by the suppressor tRNA was successfully and exclusively integrated into the protein. In the 'read-through/reaminoacylation' test, the UAG mutant mRNA was introduced with (1) no tRNA, (2) tRNA THG73 that was not charged with any amino acid or (3) tRNA THG73 enzymatically ligated with dinucleotide dCA. Lack of currents in these experiments validated the reliability of the nonsense suppression experiments.

Single-channel characterization of α4β2. Single-channel recording was performed in the cell-attached configuration on devitellinized *Xenopus laevis* oocytes at 20 ± 2 °C with a pipette potential of +100 mV, as described previously[27]. Pipettes were fabricated from thick-walled (inner diameter = 0.80 mm, outer diameter = 1.60 mm) KG-33 glass (Garner Glass Company) and coated with sylgard (World Precision Instruments); they had resistances of 10–20 MΩ. The bath solution contained 120 mM KCl, 5 mM HEPES, 1 mM $MgCl_2$ and 2 mM $CaCl_2$, pH = 7.4, so that the reversal potential for agonist-induced currents of devitellinized oocytes was ~0 mV, and the transmembrane potential of the patch was ~−100 mV. The pipette solution contained 100 mM KCl, 10 mM HEPES, 1 mM $MgCl_2$, 10 mM K_2EGTA, pH = 7.4 and was supplemented with the indicated concentrations of nicotine. Data were collected using a GeneClamp 500B amplifier (Axon Instruments) at full bandwidth (50 kHz; 4-pole Bessel, −3 dB) with a CV-5 100 GU headstage. The signal was then low-pass filtered (Avens Signal Equipment, AP220, 8-pole Bessel, −3 dB 20 kHz) and sampled with a Digidata 1320A and Clampex 9.2 (Axon Instruments) at 50 kHz. Only patches that showed no simultaneous activations were analysed. For each mutant, this was ≥3 patches from oocytes from two different donor frogs. Data were filtered offline (Gaussian, −3 dB, 5 kHz) and electrical interference at harmonics of 60 Hz was removed if necessary. Event transitions were detected with Clampfit 9.2 (single-channel search). A dead time, t_d, of 100 μs was applied to all events. Open and closed dwell time histograms were generated as described previously[31] and fitted using the predefined log-transformed exponential probability density function in Clampfit 9.2. To delineate clusters, a critical closed duration, τ_{crit}, was defined using two separate methods (Supplementary Discussion); in both cases closed dwell times longer than τ_{crit} were excluded from further analysis. Sojourns to a subconductance state (<85% of the full conductance level) were treated as closed and accounted for <10% of the total openings in all records. The time-average probability that the channel is open (P_{open}) was calculated as the total open time divided by the sum of the revised total closed time and the total open time.

31. McManus, O. B., Blatz, A. L. & Magleby, K. L. Sampling, log binning, fitting, and plotting durations of open-and-shut intervals from single channels and the effects of noise. *Pflugers Archiv-Eur. J. Physiol.* **410**, 530–553 (1987).